MOLECULAR AND CELLULAR BIOLOGY, Jan. 2011, p. 277–286 Vol. 31, No. 2
0270-7306/11/$12.00 doi:10.1128/MCB.00775-10

CARHSP1 Is Required for Effective Tumor Necrosis Factor Alpha mRNA Stabilization and Localizes to Processing Bodies and Exosomes▽§

Jason R. Pfeiffer,[1] Bethany L. McAvoy,[1] Ryan E. Fecteau,[1]† Kristen M. Deleault,[1] and Seth A. Brooks[1,2]*

Veterans Affairs Medical Center, White River Junction, Vermont 05009,[1] and Department of Medicine, Dartmouth Medical School, Lebanon, New Hampshire 03756[2]

Received 6 July 2010/Returned for modification 6 August 2010/Accepted 5 November 2010

Tumor necrosis factor alpha (TNF-α) is a critical mediator of inflammation, and its production is tightly regulated, with control points operating at nearly every step of its biosynthesis. We sought to identify uncharacterized TNF-α 3′ untranslated region (3′UTR)-interacting proteins utilizing a novel screen, termed the RNA capture assay. We identified CARHSP1, a cold-shock domain-containing protein. Knockdown of CARHSP1 inhibits TNF-α protein production in lipopolysaccharide (LPS)-stimulated cells and reduces the level of TNF-α mRNA in both resting and LPS-stimulated cells. mRNA stability assays demonstrate that CARHSP1 knockdown decreases TNF-α mRNA stability from a half-life ($t_{1/2}$) of 49 min to a $t_{1/2}$ of 22 min in LPS-stimulated cells and from a $t_{1/2}$ of 29 min to a $t_{1/2}$ of 24 min in resting cells. Transfecting CARHSP1 into RAW264.7 cells results in an increase in TNF-α 3′UTR luciferase expression in resting cells and CARHSP1 knockdown LPS-stimulated cells. We examined the functional effect of inhibiting Akt, calcineurin, and protein phosphatase 2A and established that inhibition of Akt or calcineurin but not PP2A inhibits CARHSP1 function. Subcellular analysis establishes CARHSP1 as a cytoplasmic protein localizing to processing bodies and exosomes but not on translating mRNAs. We conclude CARHSP1 is a TNF-α mRNA stability enhancer required for effective TNF-α production, demonstrating the importance of both stabilization and destabilization pathways in regulating the TNF-α mRNA half-life.

Tumor necrosis factor alpha (TNF-α) is a pleiotropic cytokine and a central mediator of inflammation. TNF-α plays a critical role in the host response to infection and injury, and the rapid, local production of TNF-α is critical to the immediate control of infection and the subsequent immune response. Overexpression of TNF-α can lead to severe tissue damage and underlies a number of disease states, including rheumatoid arthritis, Crohn's disease, and cachexia, as well as contributing to the pathologies associated with traumatic brain injury (4, 15, 18).

TNF-α biosynthesis is controlled by transcriptional and posttranscriptional mechanisms, with regulatory control points at virtually every step of its synthesis; this complex control allows for rapid, transient production (1). Posttranscriptional regulation of TNF-α operates through *cis* elements in the 3′ untranslated region (3′UTR) of the mRNA, which serve as binding sites for *trans*-acting proteins. One of the best-studied *cis* elements is the AU-rich element (ARE), which is critical in the regulation of TNF-α message nuclear export, stability, and translation (3, 4, 12, 15, 16, 24, 28). In resting cells, the TNF-α message is unstable and translationally repressed, severely limiting TNF-α protein production (3, 12, 16, 28). In response to lipopolysaccharide (LPS) stimulation, monocytes/macrophages stabilize the TNF-α message and translation is derepressed, allowing for the rapid production of TNF-α protein (3, 12, 16, 24, 28). The importance of ARE-mediated TNF-α posttranscriptional regulation was demonstrated in mice with a germ line deletion of the TNF-α 3′UTR ARE. Macrophages and T cells from these mice produced 3- to 10-fold more TNF-α protein than their wild-type counterparts, and the animals spontaneously developed pathologies indistinguishable from rheumatoid arthritis and Crohn's disease (15).

Utilizing a novel screen for TNF-α 3′UTR binding proteins, we identified calcium-regulated heat stable protein 1 (CARHSP1, also called CRHSP24) as specifically interacting with the 3′UTR of TNF-α. CARHSP1 contains a cold-shock domain with two RNA binding motifs (20, 23); cold-shock domains preferentially bind polypyrimidine regions of single-stranded RNA and DNA and regulate ribosomal translation, mRNA degradation, and the rate of transcription termination. To date, there is limited information regarding CARHSP1, with the published literature focusing primarily on the signaling pathways that phosphorylate and dephosphorylate CARHSP1 (2, 13, 17, 23, 27). These reports demonstrate that CARHSP1 is phosphorylated through the p85 phosphatidyl inositol 3-kinase (PI3K)-Akt signaling axis on Ser-53 (23). The kinase DYRK2 has also been shown to phosphorylate CARHSP1 on Ser-30, -32, and -42 *in vitro* (27). Dephosphorylation of CARHSP1 is induced by cAMP, and this process is inhibited by cyclosporine, FK506, okadaic acid, fostriecin, and calyculin A. Together, these data implicate CARHSP1 as a target of protein

* Corresponding author. Mailing address: VA Medical Center, Research 151, 215 North Main St., White River Junction, VT 05009. Phone: (802) 295-9363, ext. 5616. Fax: (802) 296-6308. E-mail: seth.brooks@dartmouth.edu.

† Present address: Case Western Reserve University, Department of Pathology, Cleveland, OH 44106.

§ Supplemental material for this article may be found at http://mcb.asm.org/.

▽ Published ahead of print on 15 November 2010.

phosphatase 2A (PP2A) and calcineurin (PP3) for dephosphorylation (2, 13).

Having identified CARHSP1 as a TNF-α 3′UTR-interacting protein, we generated stably expressing control and CARHSP1 short-hairpin RNA (shRNA) in RAW264.7 cells, a widely employed mouse macrophage cell line, to examine the effect of CARHSP1 knockdown on TNF-α mRNA and protein. These data demonstrate that the loss of CARHSP1 inhibits TNF-α protein production and reduces the level of TNF-α mRNA. mRNA stability assays with the same cell lines demonstrate that the loss of CARHSP1 decreases the TNF-α mRNA half-life in LPS-stimulated cells from a half-time ($t_{1/2}$) of 49 min to a $t_{1/2}$ of 22 min in RAW264.7 cells and decreases the stability in resting cells from a $t_{1/2}$ of 29 min to a $t_{1/2}$ of 24. Next, we examined the effect of CARHSP1 overexpression in a transient-transfection system using TNF-α 3′UTR luciferase reporters in RAW264.7 cells. CARHSP1 overexpression increases in TNF 3′UTR luciferase production in resting wild-type RAW264.7 cells but not in LPS-stimulated cells. Performing the same experiments in CARHSP1 shRNA RAW264.7 cells demonstrates that transfected CARHSP1 significantly increases TNF- 3′UTR luciferase production in LPS-stimulated cells. The effect seen in resting cells is lost if the TNF-α ARE is deleted from the 3′UTR. Further overexpression studies establish that inhibition of either calcineurin or Akt but not PP2A abolishes the increase in TNF 3′UTR luciferase expression seen with CARHSP1 overexpression. Finally, subcellular analysis of CARHSP1 demonstrates that it is a cytoplasmic protein that localizes to processing bodies and exosome granules but is not present on translating mRNAs. Together these data establish CARHSP1 as a TNF-α mRNA stability enhancer that is critical for TNF-α mRNA stabilization.

MATERIALS AND METHODS

Materials. LPS (*Escherichia coli* O26:B6), FK-506, and dimethyl sulfoxide (DMSO) were purchased from Sigma-Aldrich. Triciribine was purchased from Biomol; okadaic acid was purchased from Enzo. The following antibodies were purchased: CARHPS1 (Abcam), tubulin (Sigma), p84 (Abcam), Rrp44 (Abcam), Rrp45 (GenWay), eIF2α (StressGen), Ge-1 (Santa Cruz Bio), 4E-T (Santa Cruz Bio), and pan-actin (Neo-Markers); the anti-TTP antibody was a generous gift of William Rigby.

RNA capture assay. 293 cells (5×10^6) were plated in 150-mm tissue culture plates and transfected with 20 μg of the luciferase reporter construct pGL3-C or pGL3-TNF 3′UTR using Lipofectamine 2000. Twenty-four hours later, the cells were collected, washed twice in 4°C phosphate-buffered saline (PBS), resuspended in 500 μl of capture buffer (10 mM HEPES, 10 mM KCl, 1 mM EDTA, 1 mM EGTA, 1 mM $MgCl_2$, 1 mM dithiothreitol [DTT], 5% glycerol, 1.0 mM sodium orthovanadate, 10 μl/ml Halt protease inhibitor [Pierce, Rockford, IL], and 500 U RNase inhibitor ′Invitrogen, Carlsbad, CA]), and incubated on ice for 10 min. NP-40 was added to a final concentration of 0.25%, and the cells were pipetted up and down 20 times to lyse them, following which the nuclei were spun out at $1,500 \times g$ for 10 min at 4°C and the supernatant was used for the binding assay.

In vitro-transcribed antisense RNA was generated using the MEGAshortscript kit (Ambion) according to the manufacturer's protocol to generate a 43-nucleotide (nt) biotinylated antisense RNA complementary to the luciferase coding region and containing no predicted secondary structure at 37°C (6). The primers used to generate partially single-stranded oligonucleotides employed for *in vitro* transcription were the T7 primer (AATTTAATACGACTCACTATAGG) and the Luc primer (GTCGTCTTAATGTATAGATTTGAAGAAGAGCTGTTTC TGAGGCCTATAGTGAGTCGTATTAAATT).

For the binding reaction, 5 mg of supernatant was incubated with 100 μg of antisense RNA at 37°C for 1 h with continuous rotation. Twenty microliters packed streptavidin agarose, washed three times with capture buffer, was added to the binding reaction mixture for 30 min at 37°C with continuous rotation, following which the beads were pelleted and washed three times with capture buffer, and proteins were eluted with 200 μl of rehydration buffer (7 M urea, 2 M thiourea, 1% [wt/vol] ASB-14 detergent, 40 mM Tris base, 0.001% bromophenol blue). The protein samples were then used for two-dimensional (2D) PAGE to identify potentially relevant proteins for further analysis.

Two-dimensional gels were run using an 11-cm pH 3 to 10 immobilized pH gradient (IPG) strip (Bio-Rad, Hercules, CA) and 8 to 16% acrylamide Criterion precast gels (Bio-Rad), according to the manufacturer's specification. Following the runs, gels were stained with SilverQuest (Invitrogen) reversible silver stain according to the manufacturer's protocol, scanned with the Bio-Rad GS-800 quantitative scanner, and analyzed using the PDQuest 2D analysis software program to identify the presence or absence of proteins under different conditions. Proteins of interest were excised, subjected to in-gel tryptic digestion, and run in tandem mass spectrometry at the Dartmouth Proteomics Core, and spectra were analyzed using the Mascot analysis software program.

Immunoblotting. Cytoplasmic and nuclear fractions were generated as previously described (7). Cytoplasmic and nuclear lysates was resolved by 8-to-16%-gradient SDS-PAGE, electrotransferred to nitrocellulose, and immunoblotted with the indicated antibodies according to the manufacturer's protocol.

Generation of stable shRNA-expressing RAW264.7 cells. CARHSP1 and nontarget control shRNA plasmid constructs were purchased from Sigma-Aldrich. shRNA plasmid constructs were transfected into RAW264.7 cells using Amaxa nucleofection in accordance with the manufacturer's instructions (Lonza Walkersville Inc.). Transfected cells were incubated in standard RAW264.7 medium for 24 h and were thereafter maintained under selective pressure in RAW264.7 medium supplemented with 6 μg/ml puromycin. Clones positive for CARHSP1 knockdown were identified 2 weeks posttransfection by Western blotting for CARHSP1. Promising clones were then successively refined by two additional rounds of limiting dilution and screening by Western blotting. Nontarget control shRNA-expressing RAW264.7 cells were not cloned; rather, they were maintained as a mixed population selected based on their resistance to 6 μg/ml puromycin.

Quantification of CARHSP1 knockdown. For each Western blot, images of CARHSP1 and actin bands were captured using a gel imaging station (VersaDoc; Bio-Rad). Analysis of the images was performed using the ImageJ software program as previously described (11). Briefly, images were background subtracted using a rolling ball size of 50 pixels, and then the intensity of the CARHSP1 and actin bands was determined using ImageJ's gel analysis routine. A normalized intensity for each CARHSP1 band was calculated by dividing the CARHSP1 intensity by the actin intensity. Relative intensity for a given experimental condition was calculated by dividing the actin normalized intensity by the actin normalized intensity for the control condition.

Luciferase vectors. pGL3-Control (Promega) is the backbone vector. First, the intron from the 5′UTR of pRL-SV40 was amplified by PCR and clones into the 5′UTR of pGL3-Control-Intron, which was cut with AvrII and HindIII. pGL3-TNF 3′UTR-Intron contains the complete mouse TNF 3′UTR: nucleotides 865 to 1619 cloned into the XbaI site in the pGL3-Control-Intron vector. pGL3-ARE-Del-Intron contains TNF 3′UTR nucleotides 865 to 1283 and 1354 to 1619, generated using Quikchange (Stratagene) and the pGL3-TNF-3′UTR-Intron vector.

Transient transfections and luciferase assays. RAW 264.7 cell transfections were performed in triplicate at least 5 times ($n = 5$) using Lipofectamine LTX according to the manufacturer's protocol for RAW264.7 cells. Briefly, 125,000 RAW cells were plated in 24-well plates and allowed to rest for 24 h. Five hundred nanograms of luciferase construct and the indicated amount of mouse CARHSP1 expression vector (accession no. NM_025821; nucleotides 49 to 495) or backbone pcDNA 3.1His C vector were use for each well. Cells were lysed 24 h after transfection, and luciferase values were quantified. For each experiment, luciferase values for TNF 3′UTR luciferase expression were normalized to the effect on control luciferase expression for the specific condition. The resulting TNF-3′UTR-Intron luciferase values were expressed as a percentage of the luciferase expression with no treatment (luciferase value for condition X/luciferase value with no treatment).

mRNA quantification and stability assays. Treatment groups are indicated in the text. For RNA stability assays, actinomycin D (ActD) (5 μg/ml) was added to inhibit transcription and RNA was isolated at either 0, 30, and 60 min after ActD administration or 0, 15, and 30 min after ActD administration. Total RNA was isolated using the RNAEasy minikit with on-column DNase digestions (Qiagen) and quantified by spectrophotometry. Reverse transcription was performed using Superscript III reverse transcriptase (Invitrogen, Carlsbad, CA) on DNase-treated total RNA and oligo(dT) according to the manufacturer's protocol. Quatitative PCR was performed as previously described using the Sybr green

PCR core kit (Applied Biosystems, Foster City, CA) and a three-step reaction: 94°C for 30 s, 55°C for 30 s, and 72°C for 30 s (19). Mouse TNF primers were previously described (9); mouse cyclophilin primers were purchased from Superarray. The mRNA half-life was calculated from the linear regression of the curve generated by plotting the $\log_{10}$ [TNF-α] as a function of actinomycin D treatment.

Sucrose density fractionation. For continuous sucrose gradient fractionation, cells were washed three times with 1× PBS and resuspended in 500 μl of the lysis buffer polybuffer (15 mM Tris-HCl [pH 7.4], 15 mM $MgCl_2$, 0.3 M NaCl, 1% Triton X-100, 0.1% [vol/vol] 2-mercaptoethanol). Cells were lysed by 20 strokes with a Teflon pestle homogenizer at 1,500 rpm and centrifuged at 12,000 × *g* for 10 min to pellet the nuclei. Postnuclear supernatant was loaded onto the top of 5 ml of a 5 to 45% continuous sucrose gradient, and the samples were centrifuged at 4°C for 2 h at 55,000 rpm in a SW55Ti rotor (Beckman). Fractions were collected manually in 500-ml aliquots, and the pellet was resuspended in 500 ml. For the 30% sucrose cushion fractionation, the above procedure was employed with a 30% sucrose replacing the 5 to 45% gradient and an equal volume of supernatant to cushion was used.

Immunocytochemistry. RAW264.7 cell immunocytochemistry was performed according to the protocol of Kedersha and Anderson (14). Processing body markers were the following: goat anti-4E-T (1:200) and mouse anti-GE-1/hedls (1:1,000). Exosome markers were the following: mouse anti-Rrp44 (1:200), rabbit anti-Rrp45 (1:500), chicken anti-CARHSP1 (1:200), and mouse anti-Xpress (1:200). The following donkey Fab fragment secondary antibodies were purchased from Jackson Research: Cy2-chicken (1:200), Cy3-goat (1:2,000), and Cy-5–mouse or -rabbit (1:200) antibody. Images were obtained using a Nikon Eclipse 80i microscope with a 60× oil objective and analyzed using the NIS-Elements BR 3.0 software program.

RESULTS

RNA capture assay. One of the limitations in the field of posttranscriptional regulation has been the inability to systematically identify proteins that interact with the 3′UTR of an intact, capped, polyadenylated mRNA transcript that has been exported from the nucleus. Utilizing the transfection of luciferase reporter vectors, we have developed an assay to capture luciferase messages containing different 3′UTRs with their associated proteins. The use of transfected vectors allows for high levels of mRNA expression as well as the use of a common biotinylated antisense RNA probe to capture the message and its associated proteins for all luciferase vectors. Transfecting cells with either the control or experimental luciferase vectors allows for identification of 3′UTR-specific interacting proteins, in this case those that interact with the TNF-α 3′UTR, while excluding proteins that interact with the control luciferase message (Fig. 1).

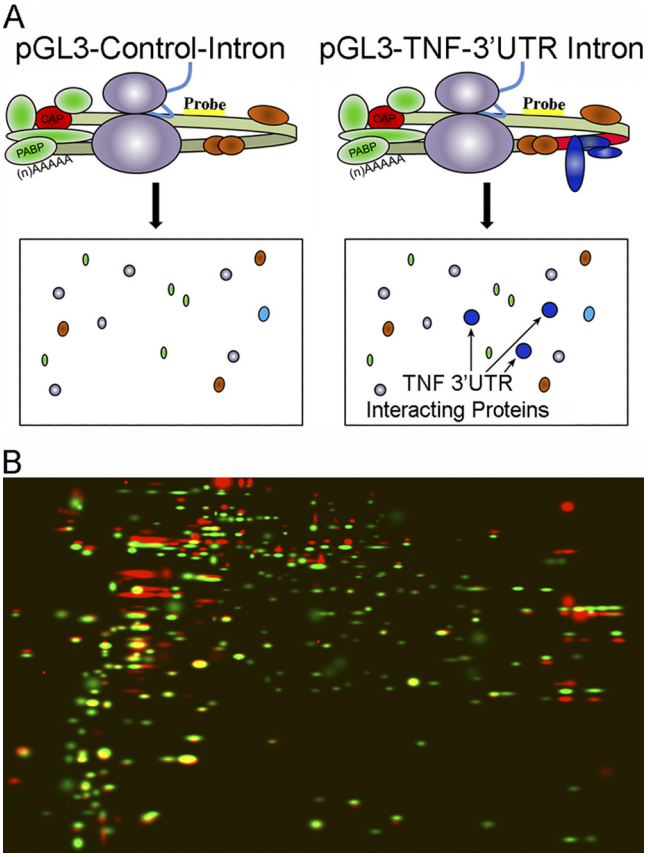

FIG. 1. RNA capture assay. (A) Schematic of the captured Control and TNF-3′UTR luciferase mRNA and the individual 2-dimensional gels. (B) Overlap of representative control luciferase (red) and TNF-3′UTR luciferase (green) RNA capture gels.

Identification of CARHSP1. Utilizing the RNA capture assay, we identified CARHSP1 as a TNF-α 3′UTR-interacting protein. Tandem mass spectrophotometry identified a 78% overlap between peptide fragments of the gel spot and CARHSP1 (Fig. 2A). CARHSP1 contains a cold-shock domain, allowing it to bind single-stranded RNA or DNA (8, 9), indicated in Fig. 2B. The mouse and human proteins are 96.6% homologous over 148 amino acid residues. Our first questions regarding a role of CARHSP1 in TNF-α posttranscriptional regulation related to its subcellular distribution and expression pattern in macrophages. Western blotting (Fig. 2C) demonstrates that CARHSP1 is confined to the cytoplasm and its expression is not altered by LPS activation of RAW264.7 cells (100 ng/ml).

Effect of CARHSP1 knockdown in RAW264.7 cells. To begin to functionally characterize the role of CARHSP1 in TNF-α expression, we generated several stable CARHSP1 shRNA-expressing RAW264.7 cell lines. Figure 3A shows the level of CARHSP1 protein knockdown in six different RAW cell lines as well as the control shRNA cells; CARHSP1 shRNA clones 1A4 and 2F2 were employed for further analysis. Quantitative densitometry of three Western blots using samples isolated on three separate days reveals a 74% reduction in CARHSP1 protein levels in clone 1A4 and a 70% reduction in CARHSP1 protein levels in clone 2F2. CARHSP1 protein knockdown by shRNA results in a significant decrease in TNF-α protein present in the culture supernatant following LPS stimulation ($P < 0.005$ at 1, 2, and 4 h), as determined by enzyme-linked immunosorbent assay (ELISA) (Fig. 3B). TNF-α expression from control shRNA and that from wild-type RAW264.7 cells are nearly identical (see Fig. S1 in the supplemental material); as with wild-type RAW264.7 cells, TNF-α protein levels from both control and CARHSP1 shRNA cells were below the level of detection in unstimulated cells. TNF-α mRNA levels were also examined in the control cells and the two CARHPS1 shRNA clones (Fig. 3C). For these studies, we employed cyclophilin as a loading control; our tests reveal that cyclophilin expression changes by less than 5% over the 4-h LPS stimulation time course. The cyclophilin primers have an efficiency of 95.7%, while the TNF-α primers have an efficiency of 97.8%, using 50 ng of starting total RNA per reaction well in 25-μl quantitative PCRs (qPCRs). LPS stimulation of the control shRNA cells results in a dramatic increase in TNF-α mRNA

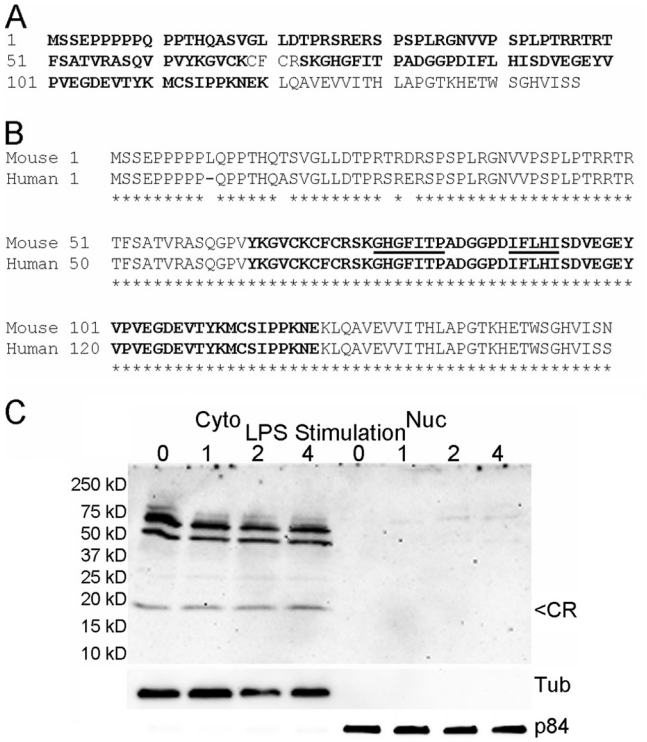

FIG. 2. CARHSP1 was identified in a screen for TNF 3′UTR-interacting proteins. (A) Tandem mass spectrometry of a putative TNF 3′UTR-interacting protein identified by 2D gel electrophoresis resulted in a 78% overlap with CARHSP1, bold sequence. (B) Mouse and human CARHSP1 share 96.6% identify over 148 residues. The bold areas indicate the cold-shock domain; the underlined areas are the predicted RNA binding domains. (C) Time course of CARHSP1 expression in resting and LPS-stimulated RAW264.7 cells. Western blotting for CARHSP1 demonstrates localization to the cytoplasm but not the nucleus. Tubulin (Tub) serves as a cytoplasmic loading control, while the nuclear matrix protein p84 serves as a nuclear loading control.

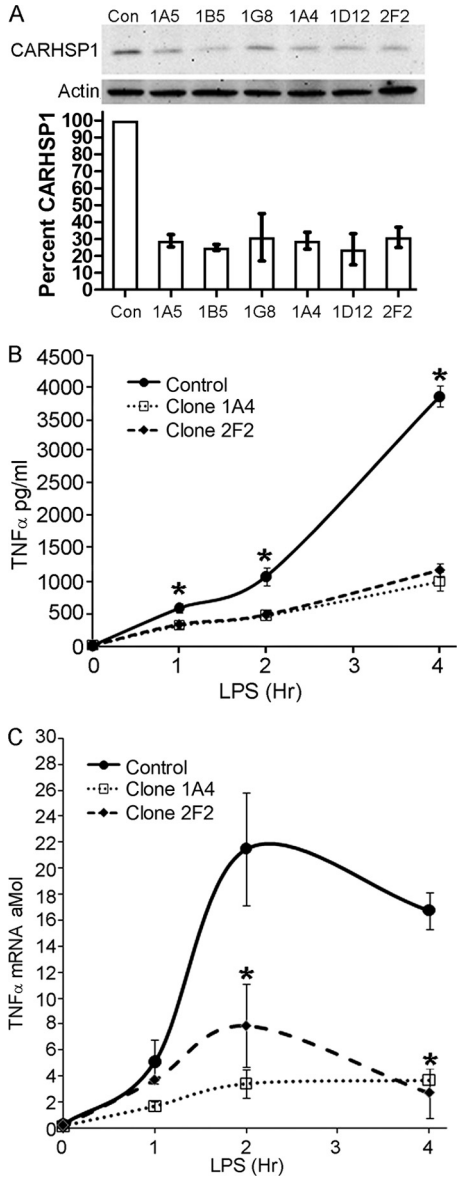

FIG. 3. CARHSP1 knockdown reduces TNF-α protein expression and mRNA levels. (A) Using either a control or a CARHSP1 shRNA, stable shRNA-expressing RAW264.7 cells were generated. Six shRNA CARHSP1 clones were screened by Western blotting for altered CARHSP1 expression. Densitometric quantification of three separate Western blots with 3 biologic replicates demonstrates CARHSP1 knockdown of 70 to 74% for the six clones. (B) Knockdown of CARHSP1 protein expression, clones 14A and 2F2, results in a significant decrease ($P < 0.005$) in TNF-α protein released into the supernatant at 1, 2, and 4 h post-LPS addition compared with control shRNA cell TNF-α expression, as determined by ELISA. (C) TNF-α mRNA levels are significantly reduced in CARHSP1 shRNA RAW264.7 cells compared with those in control shRNA RAW264.7 cells at 2 and 4 h of LPS stimulation ($P < 0.02$), as quantified by quantitative PCR.

levels, peaking at about 2 h and then beginning to decline. In contrast, TNF-α mRNA levels are significantly reduced in the CARHSP1 shRNA clones ($P < 0.02$ at 2 and 4 h LPS). Thus, loss of CARHSP1 reduces both TNF-α mRNA and protein levels in RAW264.7 macrophages, implying that CARHSP1 regulates the stability of the TNF-α message rather than regulating TNF-α translation, which should alter protein but not message levels.

CARHSP1 stabilizes TNF-α mRNA. To confirm that CARHSP1 regulates TNF-α mRNA stability, we performed stability assays using the control shRNA cells and CARHSP1 shRNA clone 2F2. The TNF-α mRNA half-life following 2 h of LPS stimulation is 49 min in the control shRNA cells and 22 min in the CARHSP1 shRNA cells. At both the 30-min time point and the 60-min time point, the remaining TNF-α message in the CARHSP1 shRNA cells is significantly reduced compared to that in the control shRNA cells ($P < 0.01$). Initial studies with RNA isolated from unstimulated clone 2F2 cells provided too little TNF-α mRNA to quantify over the time course of the stability assay. In order to obtain sufficient signal, the reaction volume for the qPCRs was increased to 50 μl and 250 ng of starting total RNA was used per well. This increased the signal sufficiently to perform stability assays; however, we did not observe a difference in TNF-α mRNA stability between the control shRNA and CARHSP1 shRNA cells. Interestingly, more TNF-α mRNA was present in the control shRNA cells

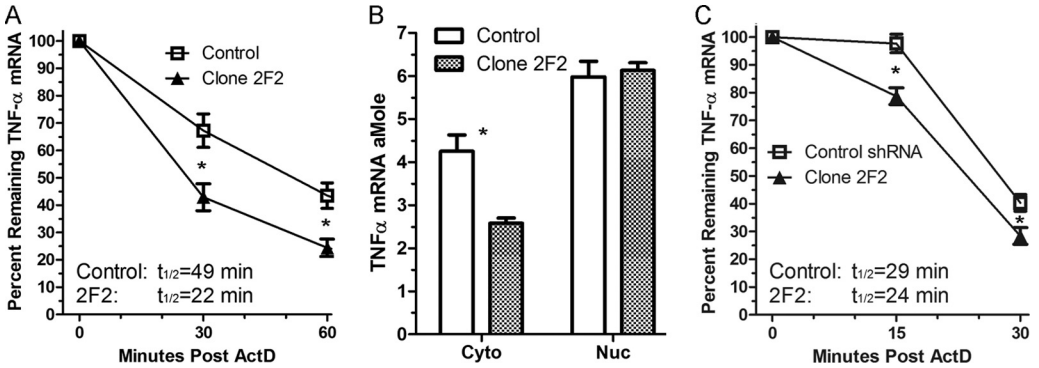

FIG. 4. CARHSP1 knockdown reduces TNF-α mRNA stability. mRNA stability assays were performed in resting and LPS-stimulated control and clone 2F2 shRNA RAW264.7 cells. mRNA was isolated at the indicated time points following the addition of the transcriptional inhibitor ActD (5 μg/ml). (A) Knockdown of CARHSP1 results in a decrease in TNF-α mRNA half life from $t_{1/2}$ = 49 min to $t_{1/2}$ = 22 min following 2 h of LPS treatment, with a significant reduction in the percentage of remaining TNF-α mRNA at 30 min and 60 min ($P < 0.01$). (B) Fractionation of control and CARHSP1 shRNA cells into cytoplasmic and nuclear compartments and quantification of TNF-α mRNA levels in each. Nuclear fractions have almost identical TNF-α mRNA levels, while TNF-α levels are significantly reduced in the cytoplasm of CARHSP1 shRNA cells ($P < 0.02$). (C) Knockdown of CARHSP1 results in a decrease in the TNF-α mRNA half-life from $t_{1/2}$ = 29 min to $t_{1/2}$ = 24 min in the cytoplasmic fraction of resting cells, with a significant reduction in the percentage of remaining TNF-α mRNA at 15 min and 30 min ($P < 0.05$).

than in the CARHSP1 shRNA cells at time zero of the stability assay (data not shown).

The lack of an effect of CARHSP1 knockdown on TNF-α mRNA stability in resting cells but difference in basal TNF-α mRNA levels is somewhat paradoxical, particularly given the cytoplasmic localization of CARHSP1, which presumably precludes the protein from functioning as a transcription factor. Given the extremely low levels of TNF-α mRNA in resting cells and the restriction of CARHSP1 to the cytoplasm, we postulated that the pool of TNF-α RNA in the nucleus might make the TNF-α mRNA appear more stable in the CARHSP1 shRNA cells, since stability assays utilize the percent remaining message. To test this, we fractionated resting control and CARHSP1 shRNA cells into cytoplasmic and nuclear compartments and compared the amount of RNA present in each fraction (Fig. 4B). The effectiveness of fractionation is demonstrated in Fig. 2C. The amounts of TNF-α RNA present in the nuclei of control and CARHSP1 shRNA cells are nearly identical (5.98 amol in control cells and 6.13 amol in CARHSP1 cells). In contrast, there is significantly more TNF-α mRNA in the cytoplasm of control cells (4.25 amol) than in CARHSP1 shRNA cells (2.58 amol) ($P < 0.02$). For these experiments, equal total starting RNA was employed; thus, these data do not indicate the precise cellular ratio of cytoplasmic to nuclear TNF-α message. However, we can conclude that the nuclear fraction of TNF-α message is not trivial and the contribution of the nuclear TNF-α RNA to the apparent half-life of the TNF-α message is greater in CARHSP1 shRNA cells, likely making the message appear more stable. This effect is likely less relevant in the LPS-stimulated cells due to the large increase in TNF-α mRNA, the inhibition of TNF-α mRNA decay pathways, and changes in the export of the TNF-α message from the nucleus (10, 24).

To confirm these findings, we performed stability assays with control and CARHSP1 shRNA cells, using RNA isolated from the cytoplasmic fraction. For the cytoplasmic stability studies, the time course was shortened to 30 min from 60 min to ensure sufficient TNF-α message was present to quantify. Cytoplasmic TNF-α mRNA half-life in the Control shRNA cells was 29 min, while the cytoplasmic TNF-α mRNA half life in the CARHSP1 shRNA cells was 24 min. There was significantly less remaining TNF-α mRNA at both the 15-min and 30-min time points ($P < 0.05$). Together, these data demonstrate that CARHSP1 regulates TNF-α mRNA stability in both resting and LPS-stimulated macrophages.

Overexpression of CARHSP1 in RAW264.7 cells. Next, we cloned the full-length coding region of mouse CARHPS1 into an expression vector and performed transient transfections utilizing a well-established system that we have previously employed in a number of studies to examine the regulation of TNF-α by tristetraprolin (TTP) (6, 7, 9, 22, 24). To establish the optimal concentration of the CARHSP1 expression construct, initial studies employed either pGL3-Control-Intron or pGL3-TNF-3′UTR-Intron luciferase reporter constructs (24) and increasing amounts of the CARHSP1 expression vector. Figure 5A demonstrates that increasing amounts of CARHSP1 have no effect on luciferase expression from the control vector in either resting or LPS-stimulated RAW264.7 cells. Figure 5B shows the effect of increasing CARHSP1 expression on TNF 3′UTR luciferase expression. In resting RAW264.7 cells, there is a dose-dependent increase in TNF 3′UTR luciferase expression, with a maximal and statistically significant effect at 100 ng ($P < 0.01$). The 27% increase in TNF 3′UTR luciferase expression is physiologically comparable to the change in TNF 3′UTR luciferase expression seen with the TNF mRNA stability regulator TTP (9), one of the best-characterized post-transcriptional regulators.

In contrast to the results seen in resting RAW264.7 cells, overexpression of CARHSP1 followed by LPS stimulation (2 h, 100 ng/ml) results in a nonsignificant decrease (9%) in TNF 3′UTR luciferase expression. Figure 5C shows CARHSP1 in RAW264.7 cells transfected with 100 ng of CARHSP1 expression vector; pcDNA3.1 HisC encodes a His and Xpress epitope at the amino end of the protein which adds about 6 kDa to the protein. Figure 5D demonstrates that the TNF-α ARE is required for the CARHSP1 cotransfection effect. The increase

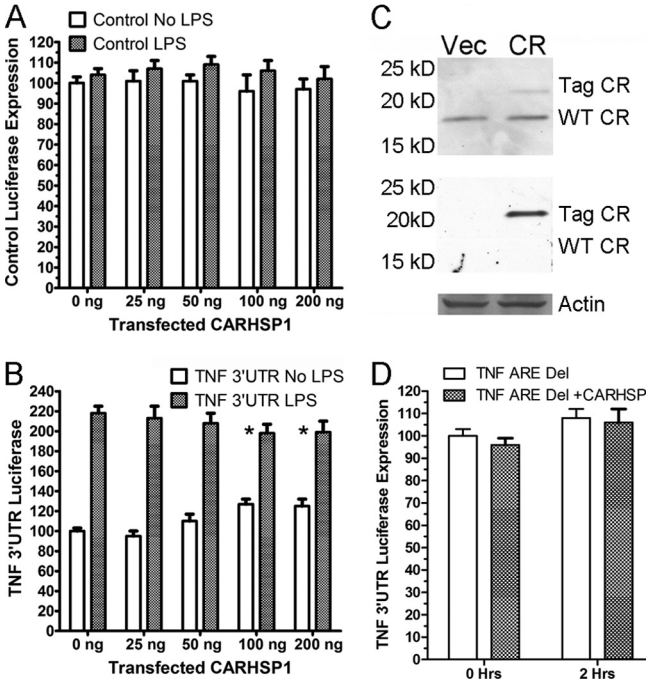

FIG. 5. The effect of CARHSP1 overexpression on TNF 3′UTR-mediated luciferase expression. Mouse CARHSP was cloned into pcDNA3.1 His-C and used for transfections into RAW264.7 cells with different luciferase reporter vectors. (A) Effect of increasing CARHSP1 transfection on pGL3-Control-Intron luciferase expression in resting and LPS-stimulated (2 h) RAW264.7 cells. There is no significant effect of CARHSP1 transfection on control luciferase expression. (B) Effect of increasing CARHSP1 transfection on pGL3-TNF 3′UTR-Intron luciferase expression in resting and LPS-stimulated (2 h) RAW264.7 cells. One hundred nanograms of transfected CARHSP1 has the maximal effect at the lowest dose, resulting in a significant increase ($P < 0.01$) in TNF 3′UTR luciferase expression in resting cells. There was no effect of transfected CARHSP1 in LPS-stimulated cells. (C) Expression of 100 ng of recombinant CARHSP1 in RAW264.7 cells. Top panel, Western blot of RAW264.7 cells transfected with either pcDNA3.1 His-C or CARHSP1 pcDNA3.1 His-C blotted for CARHSP. Middle panel, Western blot identical to that in the top panel, blotted for the Xpress epitope tag encoded by pcDNA3.1 His-C. Bottom panel, middle panel membrane blotted for actin as a loading control. (D) Effect of 100 ng of CARHSP transfection on pGL3-ARE-Del-Intron luciferase expression. No significant effect of CARHSP1 transfection was seen on ARE-Del luciferase expression in either resting or LPS-stimulated RAW264.7 cells.

seen in TNF 3′UTR expression in resting RAW264.7 cells with 100 ng of CARHSP1 is absent when the TNF-ARE-Del-Intron luciferase vector, which lacks the TNF-α ARE, is employed, demonstrating that CARHSP1 posttranscriptional regulation requires the TNF-α ARE.

It is possible that in the context of LPS stimulation, when the TNF-α mRNA degradation pathways are inhibited, there is sufficient CARHSP1 protein present in RAW264.7 cells to act on the TNF-α mRNA, making the transfected protein superfluous. To test this, we performed the transfection studies with the CARHSP1 shRNA clone 1B5, again using 100 ng of either CARHSP1 expression vector or pcDNA3.1 HisC backbone. It is important to note that the CARHSP1 shRNA targets the 3′UTR of CARHSP1; the CARHSP1 expression vector lacks the CARHSP1 3′UTR, preventing shRNA targeting of the mRNA generated from the vector. In resting CARHSP1 shRNA cells (Fig. 6A), CARHSP1 transfection significantly increased TNF-α 3′UTR-mediated luciferase expression relative to that of the pcDNA3.1 HisC-transfected CARHSP1 shRNA cells ($P < 0.005$). The effect of transfected CARHSP1 in the CARHSP1 shRNA cells was significantly higher than that in the wild-type RAW cells ($P < 0.01$). In LPS-stimulated CARHSP1 shRNA RAW264.7 cells, CARHSP1 transfection results in a significant ($P < 0.01$) 39% increase in TNF-α 3′UTR luciferase expression. These findings support the hypothesis that there is sufficient CARHSP1 in wild-type cell to stabilize the TNF-α mRNA in the context of LPS stimulation, and they support the findings from Fig. 3 and 4.

Signaling control of CARHSP1 function. Having established that CARHSP1 overexpression enhances TNF 3′UTR luciferase expression, we next sought to establish the signaling pathways involved in modulating CARHSP1 function. Dephosphorylation of CARHSP1 is induced by cAMP, and this process is inhibited by cyclosporine, FK506, okadaic acid, fostriecin, and calyculin A; together, these data implicate CARHSP1 as a target of calcineurin (PP3) and PP2A for dephosphorylation (2, 13). The same group also demonstrated that CARHSP1 is phosphorylated at serine 53 by the PI3K-Akt pathway (2). In light of these data, we examined the effect of the calcineurin inhibitor FK506 (1 ng/ml), the PP2A inhibitor okadaic acid (10 nM), and the Akt inhibitor triciribine (1 μM) on CARHSP1 function with regard to TNF 3′UTR luciferase expression. Figure 6B shows the effect of inhibiting calcineurin, PP2A, and Akt for 135 min total in wild-type RAW264.7 cells, presented to demonstrate the specific effect of inhibition on CARHSP1 function. Okadaic acid treatment (PP2A inhibition) does not alter the CARHSP1-mediated increase in TNF-α 3′UTR luciferase expression, which remained significantly higher ($P < 0.02$). In contrast, inhibition of either calcineurin (FK-506) or Akt (triciribine) blocks the increase in TNF-3′UTR luciferase expression with CARHSP1 cotransfection.

The same experiment was performed with 2 h of LPS stimulation; cells were treated with drug or DMSO for 15 min, followed by the addition of LPS for 2 h (135 min of total drug treatment) (Fig. 6C). No significant effect on CARHSP1 function was observed with drug treatment in the context of LPS stimulation, consistent with the lack of effect seen with CARHSP1 transfection and LPS stimulation, as shown in Fig. 5B. The experiment shown in Fig. 6C was then performed using CARHSP1 shRNA cells (Fig. 6D). These data demonstrate that in the context of LPS stimulation, transfected CARHSP1 function is inhibited by FK-506 and triciribine, as it is in resting cells.

Subcellular localization of CARHSP1. In light of the posttranscriptional effect of CARHSP1, we sought to determine the subcellular distribution of the protein. Sucrose density fractionation (5 to 45%) of resting and LPS-activated RAW264.7 cell cytoplasm demonstrates that CARHSP1 is present in the light fractions, 0 to 10% sucrose (Fig. 7). In contrast, the TNF-α mRNA-destabilizing protein TTP is present through the entire gradient and pellet (22); please note that TTP levels in resting cells are low. Quantification of the RNA concentration in each fraction is presented in Fig. S2A in the supplemental material. These data demonstrate that the CARHSP1

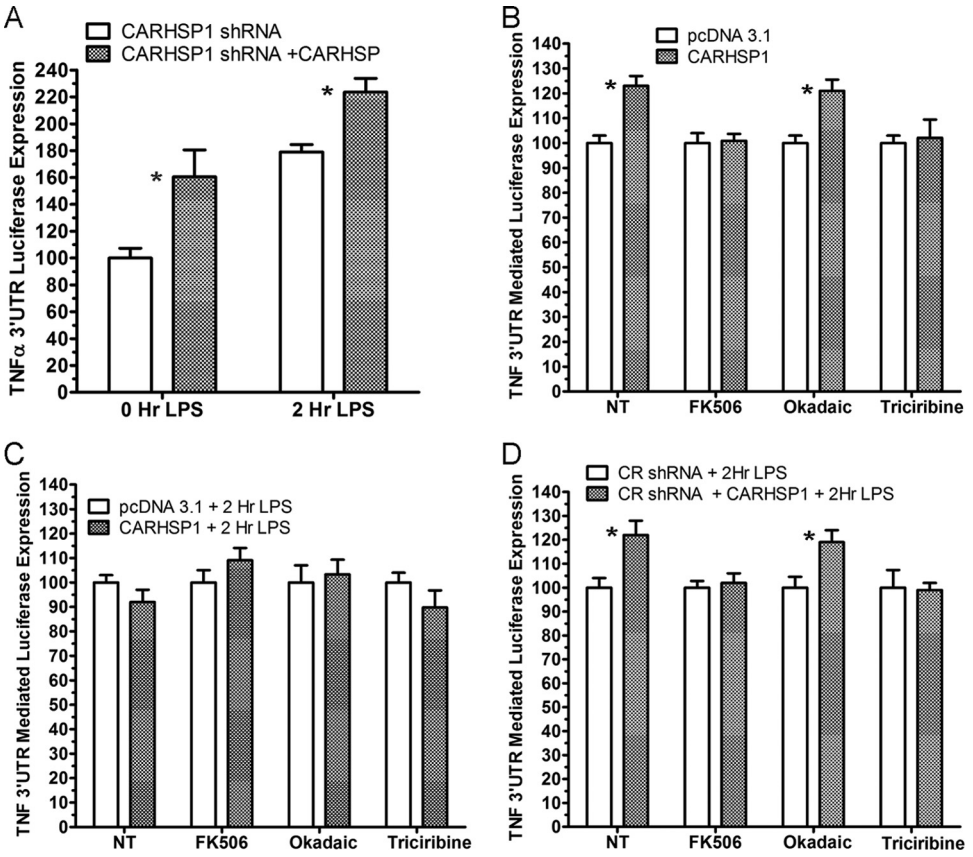

FIG. 6. The effects of calcineurin, PP2A, or AKT inhibition on CARHSP1 function. RAW264.7 cells were transfected with either pGL3-Control-Intron or pGL3-TNF-3′UTR-Intron and either 100 ng of CARHSP1 expression vector or pcDNA3.1 HIS-C. (A) Transfection of CARHSP1 shRNA clone 1B4 cells with and without LPS stimulation (2 h). Transfected CARHSP1 mediates a significant increase in TNF-α 3′UTR luciferase expression in both resting and LPS-stimulated cells ($P < 0.01$). (B) Wild-type cells were treated for 135 min total with DMSO (vehicle), FK506 (1 ng/ml), okadaic acid (10 nM), or triciribine (1 μM). TNF 3′UTR luciferase expression is normalized to the treatment effect on comparable control luciferase expression and graphed to demonstrate the effect of inhibition on CARHSP1 function. CARHSP1 transfection resulted in a significant increase in TNF 3′UTR luciferase expression with either DMSO or okadaic acid treatment ($P < 0.012$). The effect of CARHSP1 transfection is lost with FK506 and triciribine treatment. (C) Cells were treated for 15 min with DMSO (vehicle), FK506 (1 ng/ml), okadeic acid (10 nM), or triciribine (1 μM), following which LPS was added for 2 h. There were no significant effects. (D) The experiment in panel C was performed using CARHSP1 shRNA clone 1B4. The effect of CARHSP1 transfection was lost with FK506 and triciribine treatment.

protein does not dramatically shift its subcellular distribution in response to LPS. These data also confirm findings, shown in Fig. 2, that CARHSP1 protein levels do not change dramatically with LPS stimulation, again in contrast to TTP. To further clarify these data, we partitioned cytoplasmic lysate through a 30% sucrose cushion and quantified the amount of CARHSP1 protein in the pellet and supernatant (see Fig. S2B in the supplemental material). These data demonstrate that all CARHSP1 signal is present in the non-polysome-containing supernatant.

Next, we sought to determine if CARHSP1 is present in processing bodies (P-bodies). P-bodies are cytoplasmic foci containing translationally repressed mRNA; messages within P-bodies can be degraded in a 5′-to-3′ manner or stored for a return to translation (21). P-bodies lack translation factors, with the exception of eIF4E. Given the cross-reactivity of the CARHSP1 antibody seen in Fig. 2, we first established CARHSP1 immunocytochemical distribution by comparing the CARHSP1-specific antibody with the distribution of transfected CARHSP1, utilizing the Xpress tag. Figure 8A establishes that both wild-type and transfected CARHSP1 colocalizes in distinct foci in RAW264.7 cells. White arrows indicate overlapping signal; given the preponderance of overlapping signal in granules, we concluded that granules reacting with the CARHSP1 represent authentic CARHPS1 and not a cross-reactive protein.

To determine if CARHSP1 localizes to P-bodies, we employed the P-body markers 4E-T, which inhibits translation by sequestering the CAP binding protein eIF4E, and the enhancer of decapping protein Ge-1/Helds1 (14). Since macrophages express Fc receptors, we employed Fab fragment secondary antibodies. These studies demonstrate that CARHSP1 colocalizes with the P-body components in both resting (Fig. 8B) and LPS-stimulated (2 h) (Fig. 8C) cells. While a subset of the granules contain all three proteins in both resting and LPS-stimulated RAW264.7 cells, there are also granules of each protein present that do not appear to overlap with the other proteins examined. Whether the other proteins are part of the granule that is outside of the field of focus or the proteins are present in distinct subsets of granules is unclear.

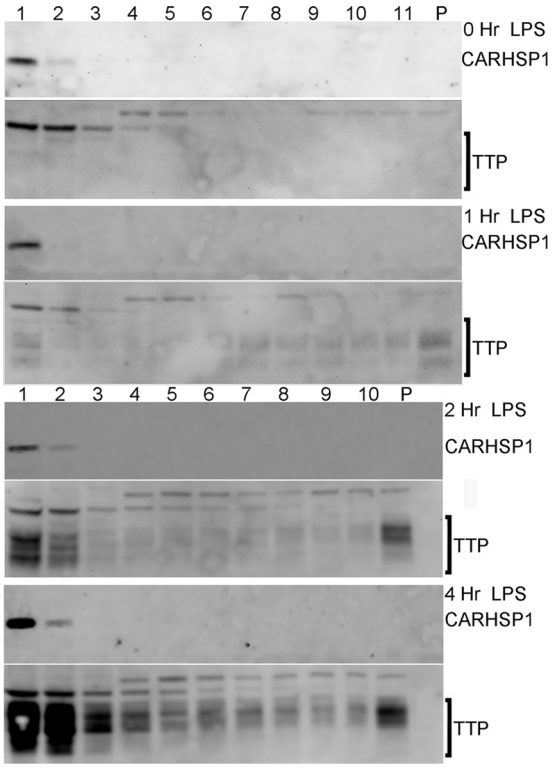

FIG. 7. CARHSP1 does not associate with actively translating mRNA. Cytoplasm from resting and LPS-stimulated RAW264.7 cells was fractionated over a continuous 5 to 45% sucrose gradient, and 500-μl aliquots were collected. Fractionated cytoplasm from 0-, 1-, 2-, or 4-h LPS-stimulated RAW264.7 cells was blotted for CARHSP1, which is present in the two lightest fractions. Following CARHSP1 blotting, the membranes were stripped and blotted for TTP. As previously reported, TTP levels increase with LPS stimulation and TTP is present thought the gradient, demonstrating fractionation.

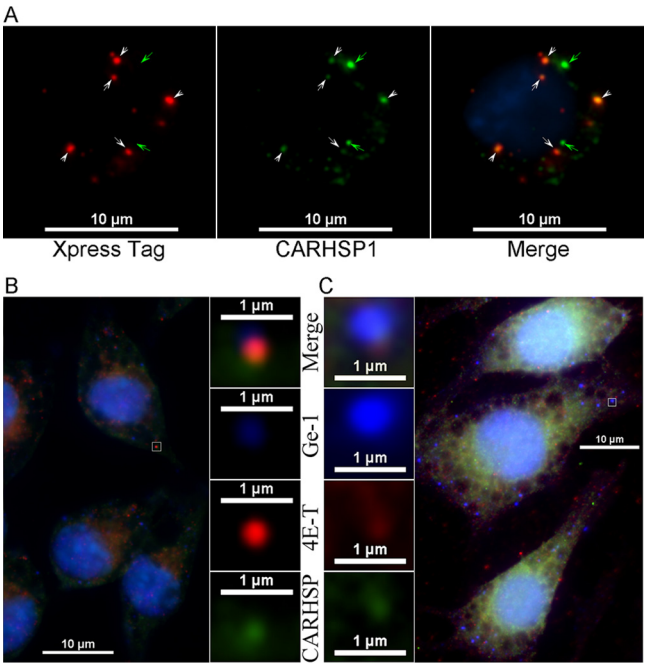

FIG. 8. CARHSP1 localizes to processing bodies. (A) Immnocytochemistry of total and transfected CARHSP1. Transfected Xpress-tagged CARHSP1 is shown in red; total CARHSP1 is shown in green. (B) CARHSP1 (green) colocalizes with the processing body markers 4E-T (red) and Ge-1 (blue) in resting RAW284.7 cells. The boxes in the center are an enlargement of the white square in the flanking panel. Note that the Ge-1 antibody cross-reacts with nuclear S6 kinase, resulting in a strong nuclear signal. (C) CARHSP1 (green) colocalizes with the processing body markers 4E-T (red) and Ge-1 (blue) in LPS-stimulated (2 h) RAW284.7 cells.

We also examined the localization of CARHSP1 with exosome granules, which are foci of exosomes degrading mRNA in a 3′-to-5′ manner. Figure 9A shows that CARHPS1 colocalizes with the structural exosome component Rrp45 as well as the cytoplasmic exosome RNase Rrp44 in resting cells. Figure 9B demonstrates the same finding in RAW 264.7 cells stimulated with LPS for 2 h. We have previously demonstrated that the P-body 5′-to-3′ RNase Xrn1 colocalizes with the exosome 3′-to-5′ RNase Rrp44 in HeLa cells (5). Given that CARHSP1 colocalizes with both P-bodies and exosome, we were interested in examining if CARHPS may link these two structures. After examining a number of cells in both resting and LPS-stimulated RAW264.7 cells, we did not find colocalization of CARHSP1 with both Ge-1 and Rrp45. We did, however, find colocalization of Ge-1 with Rrp45 in both resting (Fig. 9C) and LPS-stimulated (Fig. 9D) cells. Thus, while we cannot rule out that CARHSP1 localizes to a subset of P-body/exosome complexes, the data establish the existence of P-body/exosome complexes.

DISCUSSION

Utilizing a screen for TNF-α mRNA-interacting proteins, we identified CARHSP1 as a posttranscriptional regulator of TNF-α production specifically acting to stabilize the TNF-α message. shRNA-mediated knockdown of CARHSP1 significantly reduces TNF-α mRNA levels and protein production in RAW264.7 cells stimulated with LPS (Fig. 3), as well as TNF-α mRNA levels in resting cells (Fig. 4). TNF-α mRNA stability assays with one of the CARHSP1 shRNA clones demonstrate that the loss of CARHSP1 results in a significant reduction in the TNF-α mRNA half-life in both resting and LPS-stimulated RAW264.7 macrophages (Fig. 4). These data establish that CARHSP1 is required to maintain basal TNF-α messages levels and to fully stabilize the TNF-α message in macrophages in response to LPS stimulation. Supporting the shRNA findings, overexpression of CARHSP1 results in a significant increase in TNF-α 3′UTR luciferase production in resting cells, where the additional CARHSP1 protein acts to increase TNF-α mRNA half-life (Fig. 3). Thus, in resting cells, CARHSP1 overexpression operates to counter the dominance of the TNF-α mRNA decay pathways. Overexpression of CARHSP1 in LPS-stimulated cells, when the regulated TNF-α mRNA decay pathways are inhibited, does not produce a significant increase in TNF-α 3′UTR luciferase production (Fig. 5). However, when the same studies are performed in CARHSP1 shRNA macrophages, CARHSP1 overexpression results in a significant increase in TNF-α 3′UTR luciferase production in LPS-stimulated cells and further enhances TNF-α 3′UTR luciferase production in resting cells (Fig. 6). The finding that CARHSP1

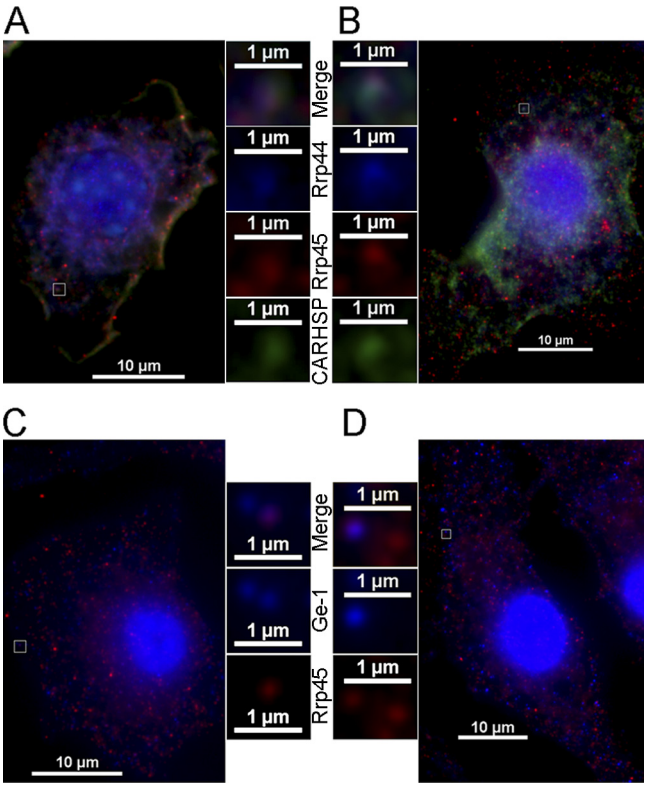

FIG. 9. CARHSP1 localizes to exosomes, and exosomes and P-bodies colocalize. (A) CARHSP1 (green) colocalizes with the exosome markers Rrp45 (red) and Rrp44 (blue) in resting RAW284.7 cells. The boxes in the center are an enlargement of the white square in the flanking panel. (B) CARHSP1 (green) colocalizes with the exosome markers Rrp45 (red) and Rrp44 (blue) in LPS-stimulated (2 h) RAW284.7 cells. (C) The structural exosome component Rrp45 (red) colocalizes with the processing body marker Ge-1 (blue) in resting RAW264.7 cells. (D) The structural exosome component Rrp45 (red) colocalizes with the processing body marker Ge-1 (blue) in LPS-stimulated (2 h) RAW264.7 cells.

protein levels are not altered by LPS stimulation (Fig. 2 and 7) supports the conclusion that there is sufficient endogenous protein to fully stabilize the TNF-α message in LPS-stimulated RAW264.7 cells. Together, these findings support the conclusion that in macrophages, the half-life of TNF-α mRNA is determined by the activities of both degradation and stabilization pathways, rather than simply being modulated by the activity of degradation pathways, and that these processes are active in both resting and LPS-stimulated cells.

Four phosphorylation sites have been identified in human CARHSP1: serines 30, 32, 41, and 52, corresponding to mouse serines 31, 33, 42, and 53. Serines 30 and 32 are dephosphorylated by increases in intracellular calcium, an event that is mediated by calcineurin (17). In contrast, serine 42 is dephosphorylated by an ionomycin-mediated calcium flux independent of calcineurin (17), while serine 52 is not dephosphorylated by increased intracellular calcium (17), indicating that this site operates independently of calcineurin. *In vivo*, serine 52 is phosphorylated by the PI3K-Akt pathway (2). Other studies have demonstrated that CARHSP1 is desphosphorylated by stimuli that increase cAMP and this process is inhibited by cyclosporine, FK506, okadaic acid, fostriecin, and calyculin A (2, 13). Our data indicate that with regard to TNF-α mRNA stability, the activities of both calcineurin and Akt (Fig. 6) are critical for CARHSP1 function. We are currently in the process of generating serine-to-alanine mutations of all four phosphorylation sites in all combinations to fully understand the role of the different sites in CARHSP1-mediated TNF-α mRNA stabilization. These studies should assist in delineating the role of the different signaling pathways involved in CARHSP1 regulation of TNF-α posttranscriptional control.

The subcellular localization of CARHSP1 is also informative. While we cannot with complete certainty exclude the possibility that a small percentage of CARHSP1 is present on the polysomes, the localization of CARHSP1 to the less-dense components of the cytoplasm, and not the nucleus, indicates that CARHSP1 is not bound to the TNF-α message when it is exported from the nucleus and that it is not associated with actively translating messages. It is also clear that LPS stimulation does not increase CARHSP1 protein levels or shift the protein onto or off the polysomes. Thus, the interaction of CARHSP1 with the TNF-α message, which clearly occurs since CARHSP1 was identified in a screen for TNF-α 3′UTR-interacting proteins, takes place following translation. This could occur either following the pioneer round of translation for messages destined for immediate decay by the standard mRNA decay pathways, such as ARE-mediated decay, or following the termination of regular translation. The association of CARHSP1 with P-bodies and exosomes, the sites of cytoplasmic mRNA decay, positions it to inhibit the decay process. We examined the cytoplasmic/nuclear localization of HuR and TTP in wild-type, control shRNA, and CARHSP1 shRNA cells but found no difference (data not shown). The finding that P-body and exosome components interact has not, to the best of our knowledge, been previously demonstrated. Given the role of each structure in different RNA decay pathways, including nonsense-, non-stop-, no-go-, and ARE-mediated decay, it is not surprising that a subset of these structures colocalize.

Recognizing that a great deal of work on the biology and biochemistry of CARHSP1 remains to be understood, our current model of CARHSP1 function is as follows. CARHSP1 interacts with the TNF-α mRNA at the sites of mRNA degradation, where it presumably prevents decay, allowing the message to enter or reenter the translating pool of mRNA; this function is regulated at least in part by calcineurin and Akt. It is possible that CARHSP1 is a component of the pathway involving HuR-mediated stabilization; however, it is also possible that CARHSP1 is part of a separate stabilization pathway in the same way that the TNF-α message is destabilized by TTP (8) and AUF1 (26) through the ARE and at least one unknown protein through the constitutive decay element (25). The data presented here demonstrate that both mRNA decay and mRNA stabilization are active, regulated processes and it is the sum of the activity of stabilization and decay that establishes the half-life of a message.

ACKNOWLEDGMENTS

This work was supported by a Veterans Administration Merit Review award to S. A. Brooks.

We thank Kelly Kieffer for critical reading of the manuscript and Michael Sporn for use of his luminometer.

REFERENCES

1. **Anderson, P.** 2000. Post-transcriptional regulation of tumour necrosis factor alpha production. Ann. Rheum Dis. **59**(Suppl. 1)**:**i3–i5.
2. **Auld, G. C., et al.** 2005. Identification of calcium-regulated heat-stable protein of 24 kDa (CRHSP24) as a physiological substrate for PKB and RSK using KESTREL. Biochem. J. **389:**775–783.
3. **Baseggio, L., et al.** 2002. Tumor necrosis factor-alpha mRNA stability in human peripheral blood cells after lipopolysaccharide stimulation. Eur. Cytokine Netw. **13:**92–98.
4. **Beutler, B., and A. Cerami.** 1989. The biology of cachectin/TNF—a primary mediator of the host response. Annu. Rev. Immunol. **7:**625–655.
5. **Brooks, S. A.** 14 May 2010. Functional interactions between mRNA turnover and surveillance and the ubiquitin proteasome system. WIREs RNA. doi: 10.1002/wrna.11.
6. **Brooks, S. A., et al.** 2002. Analysis of the function, expression, and subcellular distribution of human tristetraprolin. Arthritis Rheum. **46:**1362–1370.
7. **Brooks, S. A., J. E. Connolly, and W. F. Rigby.** 2004. The role of mRNA turnover in the regulation of tristetraprolin expression: evidence for an extracellular signal-regulated kinase-specific, AU-rich element-dependent, autoregulatory pathway. J. Immunol. **172:**7263–7271.
8. **Carballo, E., W. S. Lai, and P. J. Blackshear** 1998. Feedback inhibition of macrophage tumor necrosis factor-alpha production by tristetraprolin. Science **281:**1001–1005.
9. **Deleault, K. M., S. J. Skinner, and S. A. Brooks.** 2008. Tristetraprolin regulates TNF TNF-alpha mRNA stability via a proteasome dependent mechanism involving the combined action of the ERK and p38 pathways. Mol. Immunol. **45:**13–24.
10. **Dumitru, C. D., et al.** 2000. TNF-alpha induction by LPS is regulated posttranscriptionally via a Tpl2/ERK-dependent pathway. Cell **103:**1071–1083.
11. **Gassmann, M., et al.** 2009. Quantifying Western blots: pitfalls of densitometry. Electrophoresis **30:**1845–1855.
12. **Geppert, T. D., et al.** 1994. Lipopolysaccharide signals activation of tumor necrosis factor biosynthesis through the ras/raf-1/MEK/MAPK pathway. Mol. Med. **1:**93–103.
13. **Groblewski, G. E., et al.** 1998. Purification and characterization of a novel physiological substrate for calcineurin in mammalian cells. J. Biol. Chem. **273:**22738–22744.
14. **Kedersha, N. and P. Anderson.** 2007. Mammalian stress granules and processing bodies. Methods Enzymol. **431:**61–81.
15. **Kontoyiannis, D., et al.** 1999. Impaired on/off regulation of TNF biosynthesis in mice lacking TNF AU-rich elements: implications for joint and gut-associated immunopathologies. Immunity **10:**387–398.
16. **Kruys, V., P. Thompson, and B. Beutler.** 1993. Extinction of the tumor necrosis factor locus, and of genes encoding the lipopolysaccharide signaling pathway. J. Exp. Med. **177:**1383–1390.
17. **Lee, S., M. J. Wishart, and J. A. Williams.** 2009. Identification of calcineurin regulated phosphorylation sites on CRHSP-24. Biochem. Biophys. Res. Commun. **385:**413–417.
18. **Lenzlinger, P. M., et al.** 2001. The duality of the inflammatory response to traumatic brain injury. Mol. Neurobiol **24:**69–81.
19. **Mathews, D. H., et al.** 1999. Expanded sequence dependence of thermodynamic parameters improves prediction of RNA secondary structure. J. Mol. Biol. **288:**911–940.
20. **Nastasi, T., et al.** 1999. PIPPin is a brain-specific protein that contains a cold-shock domain and binds specifically to H1 degrees and H3.3 mRNAs. J. Biol. Chem. **274:**24087–24093.
21. **Parker, R. and U. Sheth.** 2007. P bodies and the control of mRNA translation and degradation. Mol. Cell **25:**635–646.
22. **Rigby, W. F., et al.** 2005. Structure/function analysis of tristetraprolin (TTP): p38 stress-activated protein kinase and lipopolysaccharide stimulation do not alter TTP function. J. Immunol. **174:**7883–7893.
23. **Schafer, C., et al.** 2003. CRHSP-24 phosphorylation is regulated by multiple signaling pathways in pancreatic acinar cells. Am. J. Physiol. Gastrointest. Liver Physiol. **285:**G726–G234.
24. **Skinner, S. J., et al.** 2008. Extracellular signal-regulated kinase regulation of tumor necrosis factor-alpha mRNA nucleocytoplasmic transport requires TAP-NxT1 binding and the AU-rich element. J. Biol. Chem. **283:**3191–3199.
25. **Stoecklin, G., et al.** 2003. A constitutive decay element promotes tumor necrosis factor alpha mRNA degradation via an AU-rich element-independent pathway. Mol. Cell. Biol. **23:**3506–3515.
26. **Wilson, G. M., et al.** 2003. Phosphorylation of p40AUF1 regulates binding to A + U-rich mRNA-destabilizing elements and protein-induced changes in ribonucleoprotein structure. J. Biol. Chem. **278:**33039–33048.
27. **Wishart, M. J. and J. E. Dixon.** 2002. The archetype STYX/dead-phosphatase complexes with a spermatid mRNA-binding protein and is essential for normal sperm production. Proc. Natl. Acad. Sci. U. S. A. **99:**2112–2117.
28. **Zhang, T., et al.** 2002. AU-rich element-mediated translational control: complexity and multiple activities of trans-activating factors. Biochem. Soc. Trans. **30:**952–958.